# On the Co-occurrence of Slaw-scale Bifurcation in Period-doubled Orbits in a High Order System

I. L. Daho

***Abstract*—The increase in number of state variables in a higher order systems gives rise to a new possible mode of instability which was not previously observed in simple lower-order systems. In this paper an extensive simulations were performed to capture the nonlinear behaviors of a higher order DC-DC converter described by 3D map. Floquet theory is then applied showing that: (a) two different types of bifurcations can be identified, either separately or interacting, depending on the values of bifurcation parameters (b) if there exist period 2*n* orbits created through a period doubling cascade, and if a period-*n* orbit undergoes Neimark-Sacker bifurcation, then the period-2*n* orbit also undergoes Neimark- Sacker bifurcation at the same parameter value.**

***Keywords* — Ćuk converter, current-mode control, fast-scale bifurcation, slow-scale bifurcation, chaos.**

## I. Introduction

Bifurcation of smooth dynamical systems have been extensively studied in the literature [1, 2, 3, 4]. Most of these studies address the bifurcations in lower order systems (one and two-dimensional maps) [5, 6], i.e. bifurcations that take place when one bifurcation variable is altered. These bifurcation phenomena mainly include cases of fast-scale bifurcations (flip bifurcation), and slow-scale bifurcations (Neimark-Sacker bifurcation). The dynamical of higher order systems have received relatively less research attention (three dimension map 3D) [7, 8]. In 3D systems the alteration of two bifurcation variables leads to the existence of more bifurcation possibilities. Recently an interaction of fast-scale and slow-scale phenomena has been observed in systems described by 3D maps [7, 9]. This new interaction, apart from any academic or theoretical interest, is also important from a control point of view as it describes the behavior of such systems when the dynamics of the inner and faster loop become similar to the dynamics of the outer and conventionally slower loop.

In this paper we probe the events where a flip bifurcation is followed by a Neimark-Sacker bifurcation. In the first bifurcation, the real eigenvalue becomes less than -1 and the fixed point loses stability. With further change of the parameter, if the period-doubled orbit undergoes a Neimark Sacker bifurcation, a two-loop torus develops. In order to investigate such an event, it is necessary to compute the Floquet multiplier of the period-2 orbit. Using the methodology presented in [10, 11] it is possible to calculate the eigenvalues of the period-1, and period-2 fixed points. This is often computationally involved. We show that it suffices to compute the Floquet multipliers of the unstable fixed point, because when the complex conjugate eigenvalues of this orbit move out of the unit circle, the period-2 orbit also experiences a Neimark-Sacker bifurcation at the same parameter value. If there exist period 2 orbit created through a period doubling cascade, and if a period-*n* orbit undergoes Neimark-Sacker bifurcation, then the period-2 orbit also undergoes Neimark-Sacker bifurcation at the same parameter value.

Investigation of the dynamics of a fourth order current-mode controlled Ćuk converter fully confirms the above statement. The aim is to probe into the nature of the nonlinear phenomena that can be encountered in the system when two bifurcation parameters are varied. Two different types of bifurcations can be identified, either separately or interacting, depending on the values of the bifurcation parameters.

## II. Mathematical Model of the Peak Current-Mode Controlled Ćuk Converter

The basic circuit of the closed loop current-mode controlled Ćuk converter is shown in Fig.1. The circuit represents a piecewise affine system governed by two sets of linear differential equations related to the **ON** and **OFF** switch states.

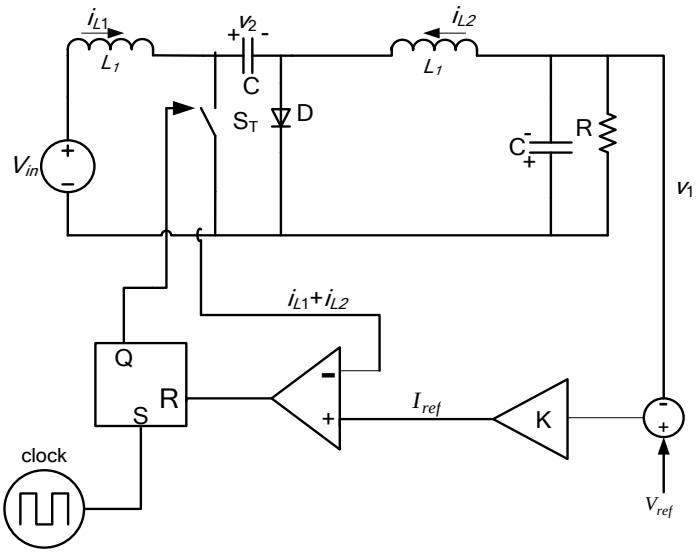


Fig.1. Schematic diagram of the closed loop current-mode controlled Ćuk converter. The nominal parameter values taken in this study are: $T$=400μs, $L_1$=$L_2$=$L$=20$mH$, $C_1$=$C_2$=$C$=47$\mu F$ K=0.6.

The author is with Electrical and Electronics Department, Sirte University, Sirte, Libya. (email Ibrahim.lameen.daho@gmail.com) .
Manuscript received June 17, 2012.

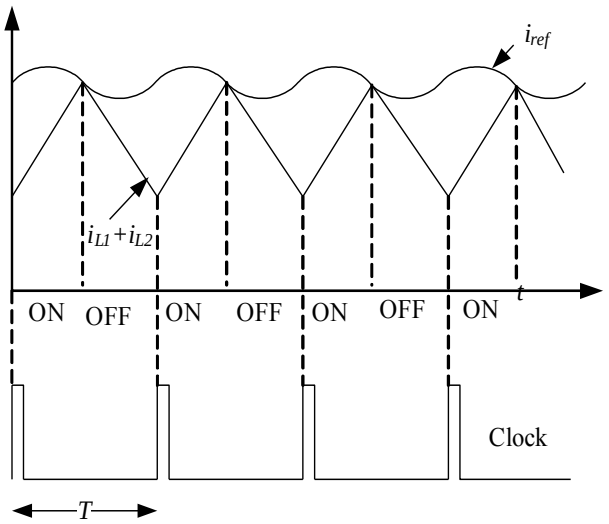


Fig.2. Generation of the ON-OFF driving signal in closed loop current-mode controlled Ćuk converter.

The **ON** state equations of the system can be written as:

$$\left.\begin{aligned} \frac{dv_1}{dt} &= \frac{i_{L2}}{C_1} - \frac{v_1}{C_1 R} \qquad \frac{dv_1}{dt} = -\frac{i_{L2}}{C_2} \\ \frac{di_{L2}}{dt} &= \frac{v_2}{L_2} - \frac{v_1}{L_2} \qquad \frac{di_{L1}}{dt} = \frac{V_{in}}{L_1} \end{aligned}\right\} \quad (1)$$

And when the switch is turned **OFF** :

$$\left.\begin{aligned} \frac{dv_1}{dt} &= \frac{i_{L2}}{C_1} - \frac{v_1}{C_1 R} \qquad \frac{dv_1}{dt} = -\frac{i_{L2}}{C_2} \\ \frac{di_{L2}}{dt} &= \frac{v_2}{L_2} - \frac{v_1}{L_2} \qquad \frac{di_{L1}}{dt} = \frac{V_{in}}{L_1} \end{aligned}\right\} \quad (2)$$

The switching signal is generated by comparing the reference current $I_{ref}$ with the sum of the two inductor currents $i_{L1}+i_{L2}$, as shown in Fig.2. As the sum of the two inductor currents reaches the reference current the switch $S_T$ turns OFF, and remains OFF until the next cycle, i.e., the switch is turned ON at the beginning of every clock period. $i_{ref}$ is generated by the output voltage feedback signal. For simplicity, a simple proportional feedback controller was used. Using a proportional-integral (PI) controller will add a fifth state to the system, further complicating the analysis of the system. The control low is given by:

$$I_{ref} = K\left(V_{ref} - v_1\right) \quad (3)$$

Where K is the control parameter and $V_{ref}$ is the reference voltage. Based on the state equations given above, a number of numerical simulations were carried out to investigate possible bifurcation behaviors that the period-1 orbit and the period-2 orbit can undergo in the closed loop current-mode controlled Ćuk converter, as two bifurcation parameters are varied. Since the input voltage and the load resistance have clear influence on the design objective and the dynamic behaviour of the system, the stability analysis of the system was carried out considering the variation of these two parameters.

### *A. Effect of Varying the Input Voltage with Load Resistance R=60 Ω*

The simulation was first performed with a relatively large value of the load resistance ($R$=60Ω) and varying input voltage $V_{in}$ from 14.5V to 17V. A typical bifurcation diagram for the closed loop current-mode controlled Ćuk converter is shown in Fig.3, using $V_{in}$ as a bifurcation parameter. It is clear that, fast-scale instability (period doubling) and interacting fast-scale and slow-scale instabilities may occur as $V_{in}$ decreases. When $V_{in}$ is large, e.g., $V_{in} \geq 16.35\,\mathrm{V}$ , the system is attracted to the period-1 orbit. As $V_{in}$ is reduced, a fast-scale instability (period doubling) begins to develop at $V_{in}$ =16.35V. When the input voltage $V_{in}$ is further reduced to 15.35V an interacting fast-scale and slow-scale bifurcation occurs (birth of two-loop torus).

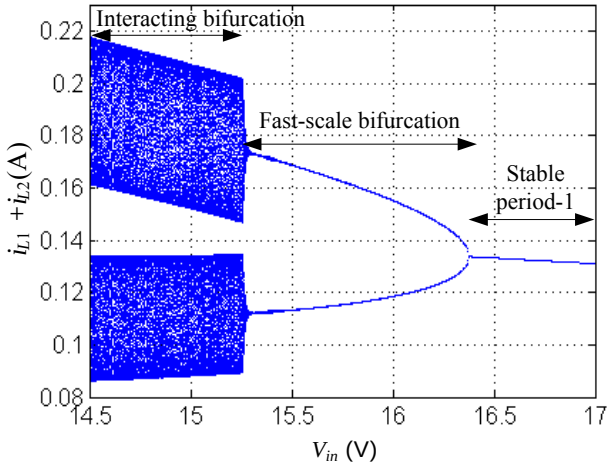


Fig.3. Bifurcation diagram, taking $V_{in}$ as bifurcation parameters ($R$=60Ω).

### *B. Effect of Varying the Input Voltage with Load Resistance R=56 Ω*

In this section, the stability of the system at smaller value of $R$ ($R$=56Ω) is studied. Similarly, we begin with a relatively large value of $V_{in}$ and observed the possible bifurcation behaviors as $V_{in}$ decreases. Fig.4 shows a typical bifurcation diagram. Unlike the above case where $R$=60Ω, the system loses its stability via a slow-scale bifurcation first before it goes into an interacting bifurcation as $V_{in}$ is reduced. When $V_{in}$ >16.45V, the system is stable. As $V_{in}$ is reduced, a slow-scale instability occurs at $V_{in}$ =16.4V. When $V_{in}$ is further reduced, e.g., $V_{in}$ =15.7V, the interacting fast-scale / slow-scale bifurcation occurs.

The above simulation results show that the closed loop current-mode controlled Ćuk converter can lose stability either via a fast-scale bifurcation or via a slow-scale bifurcation before it goes to the interacting fast-scale and slow-scale bifurcations, depending upon the values of system parameters.

ISBN: 978-988-19252-4-4
ISSN: 2078-0958 (Print); ISSN: 2078-0966 (Online)

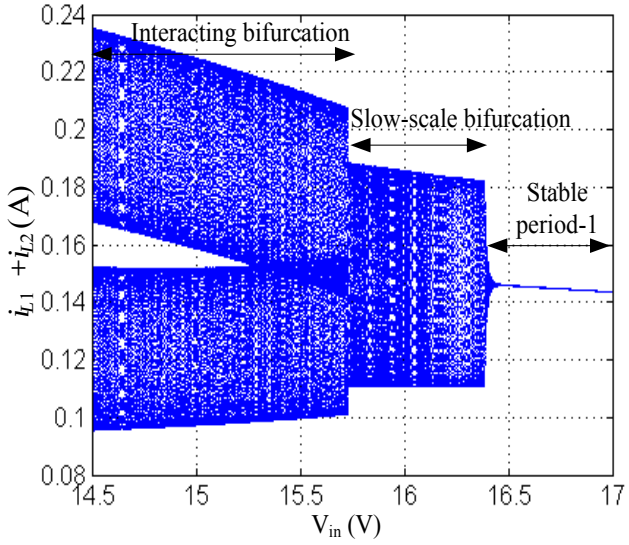


**Fig.4** Bifurcation diagram, taking $V_{in}$ as bifurcation parameters ($R$=56Ω).

## III. THEORETICAL ANALYSIS

In the normal operating condition, the state variables of the converter follow a period-1 orbit. It has been shown earlier [10, 11] that the stability of such an orbit can be assessed by computing the state transition matrix over a complete clock cycle (called the monodromy matrix), which, in turn, is composed of the state transition matrices over the ON and OFF periods and those across the switching events (called the saltation matrices). The orbit is stable if the eigenvalues of the monodromy matrix are inside the unit circle. Any crossing of the eigenvalues from the interior to the exterior of the unit circle indicates a loss of stability, i.e. a type of bifurcation occurs at that crossing point. A fast-scale bifurcation occurs when the negative real eigenvalues moves out the unit circle and a slow-scale bifurcation occurs when the complex pair of the eigenvalues moves out the unit circle. If both conditions are satisfied, an interacting bifurcation is produced.

To verify the simulation results, all possible bifurcation behaviors exhibited by the period-1 and period-2 orbits were investigated using the monodromy matrix of the system.

### *A. Derivation of the Monodromy Matrix For the period-1 orbit*

Under normal operation the system is non-autonomous, because the beginning instant of each switching cycle is defined by clock signal, so the vector field, **f** (**X**, t), is an explicit function of time.

where **X**=[$x_1$ $x_2$ $x_3$ $x_4$] and

$x_1 = v_1$ The voltage cross the capacitor $C_1$

$x_2 = v_2$ The voltage cross the capacitor $C_2$

$x_3 = i_2$ The current through the inductor $L_2$

$x_4 = i_1$ The current through the inductor $L_1$

When the system assumes a specific circuit topology, the corresponding vector field is linear and continuous. However, the vector field of the system becomes discontinuous when the switch passes from ON to OFF state and from OFF to ON state, as shown in Fig. 5.

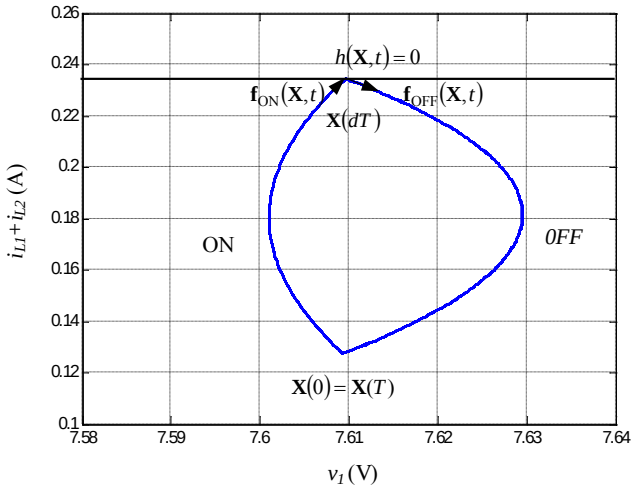


Fig.5. Period-1 orbit of the closed loop current-mode controlled Ćuk converter.

The switching condition can be represented by a switching hypersurface $h$ :

$$h(\mathbf{X},t) = \mathrm{K}(V_{ref} - x_1) - (x_3 + x_4) = 0 \tag{4}$$

The normal vector to the switching hypersurface is:

$$\mathbf{n} = \begin{bmatrix} dh(\mathbf{X},t)/dx_1 \\ dh(\mathbf{X},t)/dx_2 \\ dh(\mathbf{X},t)/dx_3 \\ dh(\mathbf{X},t)/dx_4 \end{bmatrix} = \begin{bmatrix} -1 & 0 & -1 & -1 \end{bmatrix}^T \tag{5}$$

The two vector fields before and after the switching hypersurface are:

$$\mathbf{f}_{\mathrm{ON}}(\mathbf{X},t) = \begin{bmatrix} x_3/C - x_1/CR \\ -x_3/C \\ x_2/L - x_1/L \\ V_{in}/L \end{bmatrix} \tag{6}$$

$$\mathbf{f}_{\mathrm{OFF}}(\mathbf{X},t) = \begin{bmatrix} x_3/C - x_1/CR \\ x_4/C \\ -x_1/L \\ -x_2/L + V_{in}/L \end{bmatrix} \tag{7}$$

Since the two vector fields are not equal ($\mathbf{f}_{\mathrm{ON}}(\mathbf{X}, t) \neq \mathbf{f}_{\mathrm{OFF}}(\mathbf{X}, t)$), the overall vector field of the system is discontinuous. Knowing that the OFF period lasts for (1-$d$)$T$ seconds, and the ON period lasts for $dT$ seconds, the state transition matrices for these two time intervals are:

ISBN: 978-988-19252-4-4
ISSN: 2078-0958 (Print); ISSN: 2078-0966 (Online)

$$\mathbf{\Phi}_{\text{ON}} = e^{\mathbf{A}_{\text{ON}} dT} \quad \text{and} \quad \mathbf{\Phi}_{\text{OFF}} = e^{\mathbf{A}_{\text{OFF}} (1-d)T}$$

The state transition matrix $\mathbf{\Phi}_{\text{cycle}}$ calculated over a complete cycle (the Monodromy Matrix) is defined as:

$$\mathbf{\Phi}_{\text{cycle}} = \mathbf{S}_2 \, \mathbf{\Phi}_{\text{OFF}} \, \mathbf{S}_1 \, \mathbf{\Phi}_{\text{ON}} \tag{9}$$

The saltation matrix $\mathbf{S}_1$ defines the solution on the hypersurface at $t = dT$ and is given by:

$$\mathbf{S}_1 = \mathbf{I} + \left. \frac{\left(\mathbf{f}_{\text{ON}}(\mathbf{X},t) - \mathbf{f}_{\text{OFF}}(\mathbf{X},t)\right)\mathbf{n}^T}{\mathbf{n}^T \mathbf{f}_{\text{OFF}}(\mathbf{X},t)} \right|_{t=dT} \tag{8}$$

The second saltation matrix $\mathbf{S}_2$ relates to the switching from an OFF state to an ON state and at the end of the clock cycle turns out to be an identity matrix, since the rising edge of the clock forces the switch to turn ON, i.e. both the original and perturbed orbits are forced to cross the switching hypersurface at the same time, and hence there is no need for a station matrix to describe the switching at $t=T$.

Then if $\mathbf{S}_1$ is known, it is possible to calculate out the eigenvalues of monodromy matrix of the system.

### *B. Derivation of the Monodromy Matrix For the period-2 orbit*

Fig.7 shows a stable period-2 limit cycle of the closed loop current-mode controlled Ćuk converter. It is obvious that the trajectory will cross the switching hypersurface $h$ two times in $t \in (0,\ 2T)$. In this case the system starts the clock cycle in the ON state which continues for a period of $dT$. The switch turns OFF and remains OFF until the next clock cycle. Then the switch turns ON for a period of $d_1T$, after which the switch turns OFF again. It remains OFF until the end of the second switching period, when it is turned ON again. Thus, the monodromy matrix for the period-2 orbit can be described by the same expressions used for the period-1 orbit, but with a period of $2T$. The state transition matrix over the complete cycle will be composed of the transition matrices over the four time intervals, and the four saltation matrices for the switching from an ON state to an OFF state ($\mathbf{S}_1$ and $\mathbf{S}_2$) and that from an OFF state to an ON state ($\mathbf{S}_2$ and $\mathbf{S}_4$):

$$\mathbf{\Phi}_{\text{cycle}}(2T,0) = \mathbf{\Phi}_{\text{OFF}}(2T, d_1T) \times \mathbf{S}_3 \times \mathbf{\Phi}_{\text{ON}}(d_1T, T) \times \mathbf{S}_2 \times \mathbf{\Phi}_{\text{OFF}}(T, dT) \times \mathbf{S}_1 \times \mathbf{\Phi}_{\text{ON}}(dT, 0) \times \mathbf{S}_4$$

In calculating the saltation matrix $\mathbf{S}_1$, the switching hypersurface is:

$$h_1(\mathbf{X},t) = \left(I_{ref} - m_c t/T\right) - \left(x_3(dT) + x_4(dT)\right)$$

In calculating $\mathbf{S}_1$, the expression for the switching hypersurface is:

$$h_2(\mathbf{X},t) = \left(I_{ref} - m_c t/T\right) - \left(x_3(d_1T) + x_4(d_1T)\right)$$

So that the two switching hypersurfaces have the same normal and is given by:

$$\mathbf{n}^{\text{T}} = \begin{bmatrix} 0 & 0 & -1 & -1 \end{bmatrix}$$

With these expressions, one can obtain the two saltation matrices:

$$\mathbf{S}_1 = \mathbf{I} + \left. \frac{\left(\mathbf{f}_{\text{OFF}}(\mathbf{X},t) - \mathbf{f}_{\text{ON}}(\mathbf{X},t)\right)\mathbf{n}^{\text{T}}}{\mathbf{n}^T \mathbf{f}_{\text{ON}}(\mathbf{X},t)} \right|_{t=dT},$$

$$\mathbf{S}_3 = \mathbf{I} + \left. \frac{\left(\mathbf{f}_{\text{OFF}}(\mathbf{X},t) - \mathbf{f}_{\text{ON}}(\mathbf{X},t)\right)\mathbf{n}^{\text{T}}}{\mathbf{n}^T \mathbf{f}_{\text{ON}}(\mathbf{X},t)} \right|_{t=d_1T}$$

$\mathbf{S}_2$ and $\mathbf{S}_4$ are identity matrixes for the same reasons explained in analysing the period-1 orbit.

### *C. Evaluation of the Floquet Multipliers*

The Floquet multipliers for the stable period-1 orbit and the stable period-2 orbit with variation of the input voltage $V_{in}$ were calculated for two different values of the load resistance $R$.

TABLE I
FLOQUET MULTIPLIERS OF THE PERIOD-1 ORBIT FOR VARIOUS $V_{in}$; $R$=60Ω

| $V_{in}$ (V) | eigenvalues | | | Remarks |
|---|---|---|---|---|
| | Real eigenvalues | | Modulus (Complex Pair) | |
| 16.5 | -0.9952 | 0.1996 | 0.9996 | Stable period-1 |
| **16.35** | **-1.003** | **0.2006** | **0.99968** | **Fast-scale instability** |
| 16 | -1.0151 | 0.2026 | 0.9997 | Fast-scale instability |
| 15.5 | -1.0363 | 0.2056 | 0.9999 | Fast-scale instability |
| **15.35** | **-1.0451** | **0.2068** | **1.00006** | **Interacting bifurcation** |

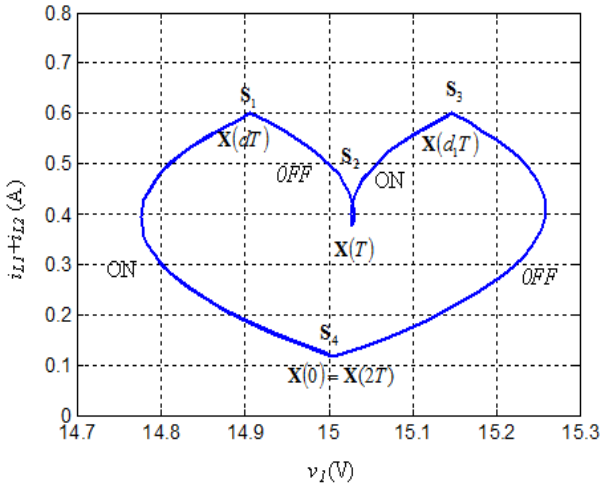


Fig.6. Period-2 orbit of the closed loop current-mode controlled Ćuk converter.

ISBN: 978-988-19252-4-4
ISSN: 2078-0958 (Print); ISSN: 2078-0966 (Online)

TABLE II

FLOQUET MULTIPLIERS OF THE PERIOD-2 ORBIT FOR VARIOUS $V_{in}$ ; $R$=60Ω

| $V_{in}$ (V) | eigenvalues | | | Remarks |
|---|---|---|---|---|
| | Real eigenvalues | | Modulus (Complex Pair) | |
| 16.35 | 0.9877 | 0.0406 | 0.9995 | Stable period-2 |
| **15.35** | **0.8286** | **0.0474** | **1.00001** | **Slow-scale instability** |
| 15 | 0.7119 | 0.0537 | 1.0004 | Slow-scale instability |

TABLE III

FLOQUET MULTIPLIERS OF THE PERIOD-1 ORBIT FOR VARIOUS $V_{in}$ ; $R$=56Ω.

| $V_{in}$ (V) | eigenvalues | | | Remarks |
|---|---|---|---|---|
| | Real eigenvalues | | Modulus (Complex Pair) | |
| 16.5 | -0.9937 | 0.1981 | 0.9999 | Stable period-1 |
| **16.4** | **-0.9976** | **0.1987** | **1** | Slow-scale instability |
| **15.7** | **-1.0218** | **0.2010** | **1.0002** | **Interacting bifurcation** |
| 15.5 | -1.0345 | 0.2040 | 1.0004 | Interacting bifurcation |

TABLE IV

FLOQUET MULTIPLIERS OF THE PERIOD-2 ORBIT FOR VARIOUS $V_{in}$ ; $R$=56Ω.

| $V_{in}$ (V) | eigenvalues | | | Remarks |
|---|---|---|---|---|
| | Real eigenvalues | | Modulus (Complex Pair) | |
| **15.7** | **0.8827** | **0.0431** | **1.0003** | **Slow-scale instability** |
| 15.5 | 0.8642 | 0.0466 | 1.0009 | Slow-scale instability |
| 15 | 0.7189 | 0.0531 | 1.0013 | Slow-scale instability |

The results are shown in Tables I, II, III and IV. Tables I and II show the Floquet multipliers of the stable period-1 orbit and the stable period-2 orbit, respectively, for $R$=60 Ω.

By reducing the load resistance to R=56Ω a different bifurcation scenario is obtained. Tables III and IV show the Floquet multipliers of the stable period-1 orbit and the stable period-2 orbit, respectively, for $R$=56Ω. In this case the system goes from period-1 to an interacting bifurcation via a slow-scale bifurcation at 16.4V, and then the period-1 orbit undergoes a period doubling bifurcation (fast-scale bifurcation at 15.7V.

In this case, when the period-2 orbit is born it is already unstable with complex eigenvalues with magnitude greater than 1, as can be seen in Table IV.

From the above analysis it is clear that when the period-1 orbit losses stability through a slow-scale bifurcation (Neimark-Sacker bifurcation) the period-2 orbit will also undergo a loss of stability.

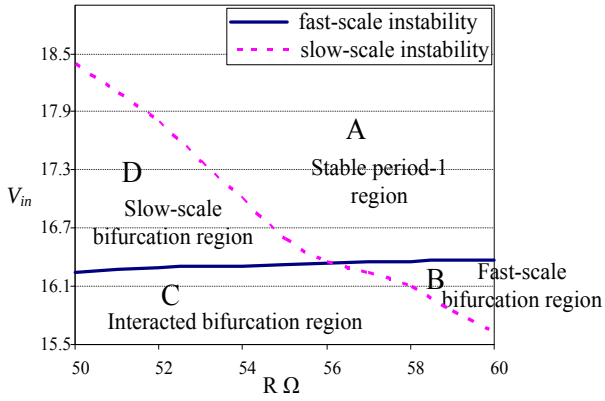


Fig. 7. Bifurcation lines in the parameter plane ($R$, $V_{in}$).

### *D. The Two-parameter Bifurcation Lines in Vin and R Parameter Space*

It is clear from the previous sections that different combinations of circuit parameter values can lead to different ways for the system to loss its stability. Therefore, it is important to obtain the bifurcation lines for the fast-scale bifurcation (when the negative real eigenvalues moves out the unit circle) and the slow- scale bifurcation (when the complex pair of the eigenvalues moves out the unit circle) in the $V_{in}$ and $R$ parameter plane. Using the eigenvalues of the monodromy matrix, the stability of the system was investigated for different values of the input voltage and the load resistance. In particular, the load resistance $R$ was varied in the range (50Ω-60Ω) and for each value the critical value of $V_{in}$ was calculated for which either, a slow-scale or a fast-scale instability occurs. The other parameters were fixed. The two-parameter bifurcation lines computed analytically are shown in Fig. 7. The two lines divide the parameter plane into four regions; stable operation (region **A)**, fast-scale instability (region **B)**, interacting bifurcation (region **C)**, and slow-scale instability (region **D)**. Fig. 7 shows that when $V_{in}$ decreases, the system either leave the stable region **A** via a fast-scale bifurcation (with high value of R) or via a slow-scale bifurcation (low value of R) before it goes to the interacting bifurcation region **C**, depending upon the choice of the system's load resistance value. The figure also shows that the two lines can cross at particular values of the input voltage, $V_{in} = 16.346V$, and load resistance R=56.55Ω i.e. the negative real and the complex pair of the eigenvalues move out the unit circle at the same time (Codimention-2 bifurcation node), i.e. bifurcations that take place when two bifurcation variable are altered.

It is worth mentioning that if the system operates with one bifurcation parameter value closer to codimention-2 bifurcation nodes, a very small change in the other bifurcation parameter could leads to a different type of instability. It may also mean that the system never operates in the stable region. Therefore, it is important to be able to locate such point and re-examine the stability of the system at those key values.

ISBN: 978-988-19252-4-4
ISSN: 2078-0958 (Print); ISSN: 2078-0966 (Online)

## IV. Conclusion

In conclusion, we may come out with the following general observation for the dynamical behaviour of high dimensional maps systems

1- An interacting fast-scale and slow-scale bifurcation occurs, corresponding to the simultaneous occurrence of a fast-scale bifurcation and a slow-scale bifurcation.

2- The system can lose stability via a fast-scale bifurcation, a slow-scale bifurcation, or an interacting bifurcation, depending upon the values of the system's load resistance and input voltage.

3- When a period-1 orbit undergoes a slow scale bifurcation, a period-2 orbit undergoes a similar bifurcation.

4- A codimention-2 bifurcation can take place (the fast-scale bifurcation and the slow-scale bifurcation occur at the same time) at particular values of the bifurcation parameters

5- The system may never operate in the stable region if one the bifurcation parameters is chosen just below the codimention-2 bifurcation whatever is the value of the other bifurcation parameter.

## References

[1] S. Banerjee and G. Verghese, *Nonlinear Phenomena in Power Electronics: Bifurcations, Chaos, Control, and Application*. New York: IEEE Press, 2001.

[2] M. Di Bernardo, F. Garofalo, L. Glielmo, and F. Vasca, "Analysis of chaotic buck, boost and buck-boost converters through switching maps," in *PESC Record - IEEE Annual Power Electronics Specialists Conference*, 1997, pp. 754-760.

[3] K. Chakrabarty, G. Poddar, and S. Banerjee, "Bifurcation behaviour of the buck converter," *IEEE Transactions on Power Electronics,* vol. 11, no. 3, pp. 439-447, 1995.

[4] A. E. Aroudi, L. Benadero, E. Toribio, and G. Olivar, "Hopf bifurcation and chaos from torus breakdown in a PWM voltage-controlled DC-DC boost converter," *IEEE Transactions on Circuits and Systems I: Fundamental Theory and Applications,* vol. 46, no. 11, pp. 1374-1382, 1999.

[5] S. Banerjee and C. Grebogi, "Border-collision bifurcations in two-dimentional piecewise smooth maps," Physical Review E, vol. 59, no.4, pp. 4052-4061, 1999.

[6] [60] S. Banerjee, M. S. Karthik, G. Yuan, and J. A. Yorke, "Bifurcations in one-dimensional piecewise smooth maps - theory and applications in switching circuits," IEEE Transactions on Circuits and Systems I: Fundamental Theory and Applications, vol. 47, no. 3, pp. 389-394, 2000.

[7] Y. Chen, C. K. Tse, S. C. Wong, and S. S. Qiu, "Interaction of fast-scale and slow-scale bifurcations in current-mode controlled DC/DC converters," *International Journal of Bifurcation and Chaos,* vol. 17, no. 5, pp. 1609-1622, 2007.

[8] Y. Chen, C. K. Tse, S. S. Qiu, L. Lindenmuller, and W. Schwarz, "Coexisting fast-scale and slow-scale instability in current-mode controlled DC/DC converters: Analysis, simulation and experimental results," *IEEE Transactions on Circuits and Systems I: Regular Papers,* vol. 55, no. 10, pp. 3335-3348, 2008.

[9] I. Daho, D. Giaouris, B. Zahawi, V. Pickert, and S. Banerjee, " Fast-slow scale bifurcation in higher order open loop current-mode controlled DC-DC converters," in *the second IFAC meeting related to analysis and control of chaotic systems,* (chaos09), London, United Kingdom, *June* 2009.

[10] D. Giaouris, A. Elbkosh, S. Banerjee, B. Zahawi, and V. Pickert, "Stability of switching circuits using complete-cycle solution matrices," in *Proceedings of the IEEE International Conference on Industrial Technology*, 2006, pp. 1954-1959.

[11] D. Giaouris, S. Banerjee, B. Zahawi, and V. Pickert, "Stability Analysis of the Continuous Conduction Mode Buck Converter via Filippov's Method," *IEEE Transactions on circuts and systems-,* vol. 55, no. 4, pp. 1084-1096, 2007.

ISBN: 978-988-19252-4-4
ISSN: 2078-0958 (Print); ISSN: 2078-0966 (Online)